The anatomic evaluation of the internal mammary artery using multidetector CT angiography

Bülent Karaman, Bilal Battal, Yalçın Bozkurt, Uğur Bozlar, Sait Demirkol, Mehmet Ali Şahin, Mustafa Taşar

PURPOSE
To determine the normal anatomic features and variations of the internal mammary arteries (IMAs) and to describe the relationship between the diameter and distance to the sternal edge of the IMAs, gender, and location (right-left) of the IMAs in patients who underwent multidetector computed tomography (MDCT) angiography of the thorax for various reasons.

MATERIALS AND METHODS
A total of 164 patients who underwent MDCT angiography of the thoracic vascular structures for various reasons were analyzed retrospectively. The right and left IMAs were analyzed individually, and normal anatomic features and variations were recorded. The relationships between gender, side and diameter of the IMAs, and distance to the sternal edge of the IMAs were evaluated.

RESULTS
There were 328 (164 right, 164 left) IMAs in 164 patients (110 males, 54 females; mean age, 43.96 years). A total number of five arteries (1.5%) had anatomic variation. Whereas 325 IMAs had an origin separate from the subclavian artery, three LIMA of the 328 arteries (0.91%) had a common origin with the thyrocervical trunk or costocervical trunk. Two (0.6%) IMAs (one LIMA and one RIMA) in the same patient were duplicated at the level of the first and second costal cartilage. There were no statistically significant correlations between age and diameter or between gender and diameter of the RIMA and LIMA at the origin and level of tracheal bifurcation ($P > 0.05$). Mean distance between the lateral margin of the sternum and midpoint of LIMA and RIMA were 12.42 mm and 13.00 mm, respectively.

CONCLUSION
The normal anatomic features and variations of the IMAs have an important role in cardiovascular bypass surgery, breast reconstruction, and percutaneous transthoracic procedures. MDCT angiography allows a precise and detailed evaluation of IMAs.

Key words: • internal mammary artery • tomography, spiral computed • angiography

The internal mammary artery (IMA) has become more important in recent years. First, it is one of the bypass arteries in cardiovascular surgery. The left internal mammary artery (LIMA) is the first choice in coronary artery bypass grafting because of reduced cardiac events and superior graft patency (1, 2). With their adequate size, IMAs are suitable recipient vessels for free tissue transfers, especially in breast reconstruction (3). Moreover, their anatomic descriptions are important for percutaneous transthoracic procedures, such as needle biopsy of the lung (4). Complications have been reported, although most of these procedures are performed safely (5). This area is also used for subclavian vein catheterizations. For all these reasons, it is important to be aware of all variations in the origin, branching pattern, course, and diameter of the IMA.

The IMA usually has an origin separate from the first part of the subclavian artery that is proximal to the anterior scalene muscle. This artery occasionally has a common origin with the other branches of the subclavian artery, such as the thyrocervical trunk, scapular artery, dorsal scapular artery, thyroid artery, or costocervical trunk (6–8). It first runs ventral to the pleural cupola, passing the brachiocephalic vein underneath. Then, the artery descends dorsal to the sternoclavicular joint and costal cartilages and ventral to the parietal pleura. It then runs between the transversus thoracis muscle and intercostal muscles and branches off to each intercostal space. At the end, the IMA divides into the superior epigastric artery and musculophrenic artery between the sixth and seventh costal cartilage (9–11).

Digital subtraction angiography (DSA) is regarded as the gold standard in the evaluation of vascular structures, although its invasive nature significantly limits its role. With recent advances in multidetector computed tomography (MDCT) technology, even vascular structures with very small diameters can be depicted easily, and as a consequence, the number of the invasive DSA examinations has been reduced (12–17).

The aim of this study was to evaluate the normal anatomic features and variations of the IMAs and to determine the relationship between age, gender, location (right/left), diameter, and distance to the sternal edge of the IMA in patients who underwent MDCT angiography of the thorax for various reasons.

Materials and methods

Patients

Approval for this retrospective study was obtained from our institutional review board. A total of 193 patients who underwent computed tomographic (CT) angiography of the arcus aorta and its branches for various reasons from January 2009 through February 2011 were analyzed retrospectively. Twenty-nine patients were excluded because of

From the Departments of Radiology (B.K., B.B. ✉ bilbat_23@yahoo.com, Y.B., U.B., M.T.), Cardiology (S.D.), and Cardiovascular Surgery (M.A.Ş.), Gülhane Military Medical School, Ankara, Turkey.

a history of bypass surgery (n=21) or suboptimal CT angiography examination (n=8). The remaining 164 patients (mean age, 49.36 years; range, 19–91 years) were included in our study. One hundred and ten were men (mean age, 47.42 years; range, 19–91 years) and 54 patients were women (mean age, 54.24 years; range, 21–75 years).

CT protocol

CT angiography examinations were performed using a 64-detector scanner (Aquilion 64, Toshiba Medical Systems, Otawara, Japan). In the standard CT protocol for thoracic and arcus aorta CT angiography examinations, a scanogram area from the middle cervical spine to the middle lumbar spine level in a supine position was adopted as the field of view (FOV). An 18- to 20-gauge angiocath needle was used to inject 90–130 mL of non-ionic iodinated contrast media into the patient's antecubital vein. Bolus-tracking method was used with an automatic injector at a rate of 5 mL/s and 30 mL of saline solution at a rate of 3 mL/s (Medrad Stellant D Dual Syringe CT Injection System, Indianola, Pennsylvania, USA). The region of interest was located at the proximal descending aorta, and the threshold value for CT angiography was set at 150 HU. Helical scanning was automatically initiated when the threshold was surpassed. Scan parameters were 120 kV, 300 mA, and 400 ms rotation time with a slice thickness of 0.5 mm and increments of 0.4 mm, using a detector collimation of 64×0.5 mm (pitch, 0.64).

All of the obtained axial images were transferred to a workstation. Postprocessed multiplanar-reformatted (MPR), maximum-intensity projection (MIP), and three-dimensional volume-rendering (3D VR) images were used for evaluation.

Vascular system analysis

The raw data axial images obtained by MDCT angiography and post-processed MPR and MIP and 3D VR images were evaluated by two radiologists (with three and six years of experience in cardiovascular imaging), and the decisions were made in consensus. The normal anatomy and variations in the origin of the right and left IMAs were analyzed, and the anatomic features and variations were recorded. We also evaluated the diameter of the right internal mammary artery (RIMA) and LIMA at the origin, the diameter of the RIMA and LIMA at the level of tracheal bifurcation, and the distance between the lateral margin of the sternum and the midpoint of LIMA and RIMA at the level of tracheal bifurcation in all 164 patients.

Statistical analysis

Percentage (%) for categorical data and median (min–max) values for continuous data were used in descriptive statistics. Because our study group did not show normal distribution, nonparametric tests were used. Mann-Whitney U test was used to compare male and female measures, and Wilcoxon signed rank tests were used to compare the left and right sides. Spearman rank correlation coefficients were calculated to show relationships between measures. We analyzed the data to determine the following:

1. Differences of LIMA and RIMA distances to the sternum in relation to gender and age.
2. Differences of LIMA and RIMA diameter in relation to gender and age.

Correlation among gender, side, age, the diameter of RIMA and LIMA, and the distance between the sternal edge of RIMA and LIMA were assessed with the Mann-Whitney U test and chi-square test. All statistical analyses were made using Statistical Package for the Social Sciences software (version 15.0, SPSS Inc., Chicago, Illinois, USA). *P* values less than 0.05 were accepted as significant.

Results

A total number of 328 IMAs (164 right, 164 left) were detected in 164 patients (Figs. 1 and 2). All of the IMAs arose from the first part of the subclavian arteries. A total of five arteries (1.5%) had anatomic variation. Three of the 328 arteries (0.91%), which were LIMA, had a common origin with the thyrocervical trunk (n=1) and costocervical trunk (n=2) (Fig. 3). On the other hand, the remaining 325 IMAs had an origin separate from the subclavian artery. Two (0.6%) IMAs (one LIMA and one RIMA) in the same patient were partially duplicated at the level of the first and second costal cartilage (Fig. 4).

Diameters of the origin of the LIMA and RIMA ranged from 1.4 to 3.7 mm (mean, 2.56 mm; median, 2.50 mm) and 1.2 to 4.2 mm (mean, 2.58 mm; median, 2.50 mm), respectively. Diameters of the LIMA and RIMA at the level of the tracheal bifurcation ranged from 1 to 3.3 mm (mean, 2.29 mm; median, 2.30 mm) and 1 to 3.1 (mean, 2.30 mm; median, 2.30 mm), respectively. In male and female patients, the diameters of the LIMA and RIMA at the origin and the level of the tracheal bifurcation are presented in Table 1. There were no statistically significant correlations between age and diameter and between gender and diameter of the RIMA and LIMA at the origin and level of the tracheal bifurcation (*P* > 0.05) (Fig. 5).

The distance between the lateral margin of the sternum and midpoint of LIMA and RIMA (at the level of the tracheal bifurcation) ranged from 7 to 18 mm (mean, 12.42 mm; median, 12

Table 1. The diameters of the internal mammary arteries

			Male	Female
Diameter at the origin	RIMA	Mean±SD	2.56±0.52	2.57±0.44
		Median	2.5	2.5
	LIMA	Mean±SD	2.56±0.46	2.54±0.51
		Median	2.5	2.5
Diameter at the level of the tracheal bifurcation	RIMA	Mean±SD	2.30±0.42	2.34±0.31
		Median	2.3	2.4
	LIMA	Mean±SD	2.29±0.45	2.35±0.43
		Median	2.3	2.3

RIMA, right internal mammary artery; LIMA, left internal mammary artery; SD, standard deviation.
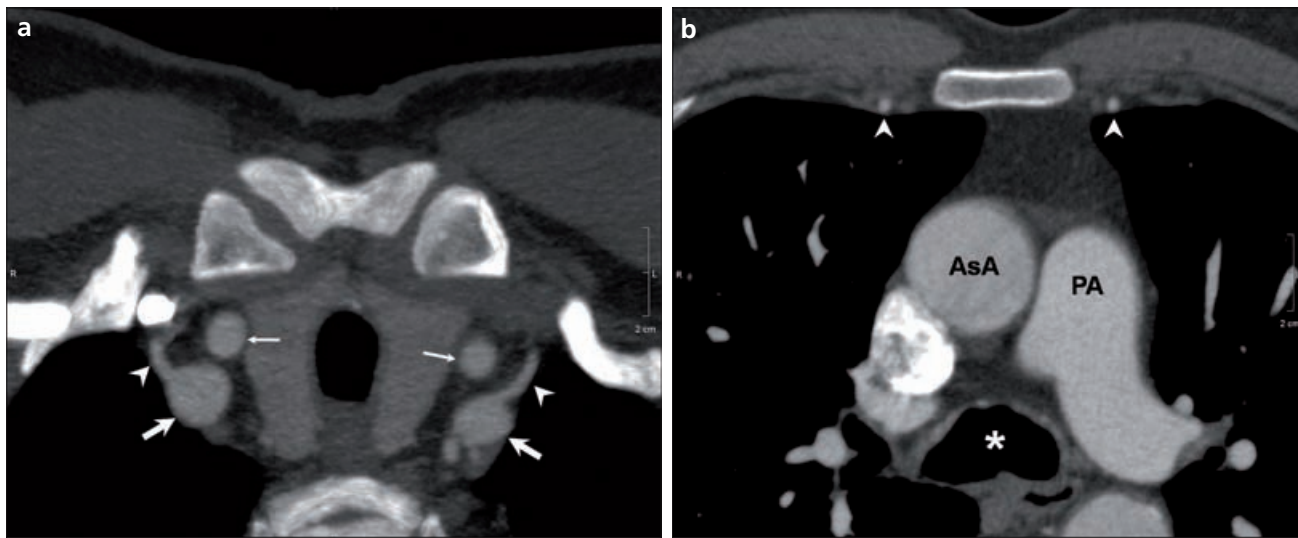
Figure 1. a–c. Axial (a, b) and coronal MIP (c) CT angiography images show origins and parasternal courses of the RIMA and LIMA *(arrowheads)* in a 46-year-old man. RIMA and LIMA arise from the right and left subclavian arteries *(thick arrows)* separately. *Thin white arrows* show right and left common carotid arteries. AsA, ascending aorta; PA, main pulmonary artery; *, tracheal bifurcation.
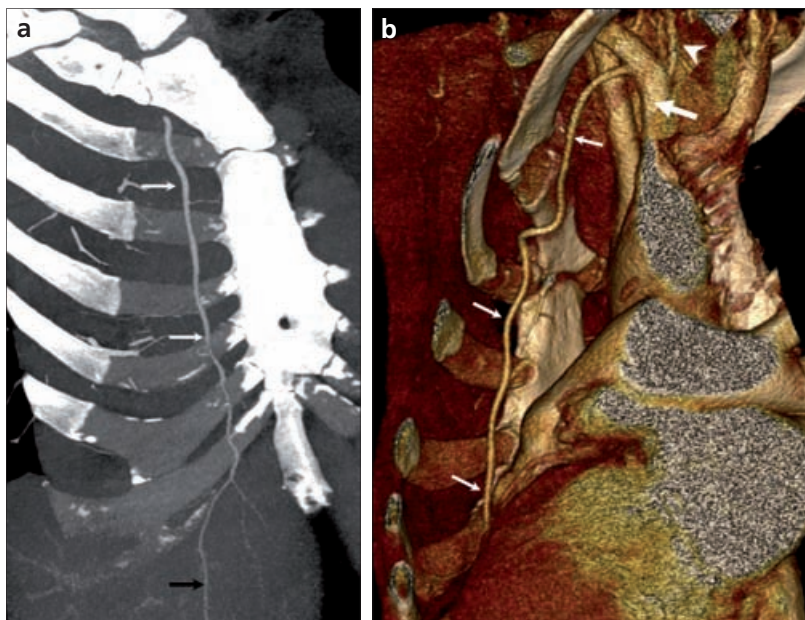
Figure 2. a, b. Oblique coronal MIP (a) and posteroanterior oblique coronal view volume rendered (b) CT angiography images show an origin and course of the IMA *(thin arrows)* that originates from the subclavian artery *(thick arrow)* and continues as the superior epigastric artery *(thin black arrow). Arrowhead* (b) shows vertebral artery.

mm) and 8 to 21 mm (mean, 13.00 mm; median, 13.01 mm), respectively (Table 2). The mean distance of RIMA from the sternal edge was calculated higher than LIMA (*P* < 0.001). There were no statistically significant correlations between age and the distance to the sternum or between gender and the distance to the sternum of the RIMA and LIMA at the level of the tracheal bifurcation (*P* > 0.05) (Fig. 6).

Discussion

In recent years, the IMA has become important for cardiovascular surgery, plastic surgery, and interventional radiology for many reasons. In evaluation of the normal anatomic features and variations of the IMAs, anatomic, angiographic, and CTA research methods have been used so far. These

Table 2. The distance between the lateral margin of the sternum and the midpoint of internal mammary arteries

		Male	Female
RIMA to sternal edge	Mean±SD	13.26±2.50	12.47±2.87
	Median	13	13
LIMA to sternal edge	Mean±SD	12.79±2.38	11.67±2.46
	Median	13	12

RIMA, right internal mammary artery; LIMA, left internal mammary artery; SD, standard deviation.
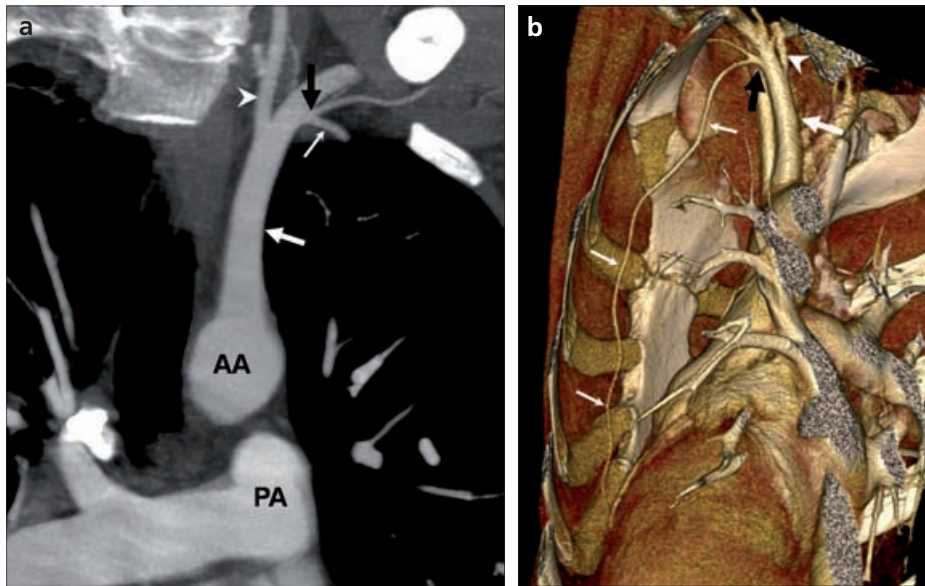
Figure 3. a, b. Oblique coronal MIP **(a)** and posteroanterior oblique coronal view volume rendered **(b)** CT angiography images show that the origin and course of the LIMA *(thin white arrows)* arise from the left subclavian artery *(thick white arrows)* as a common trunk with costocervical trunk *(black arrows)* in a 49-year-old man. *Arrowheads* show left vertebral artery. AA, arcus aorta; PA, pulmonary artery.
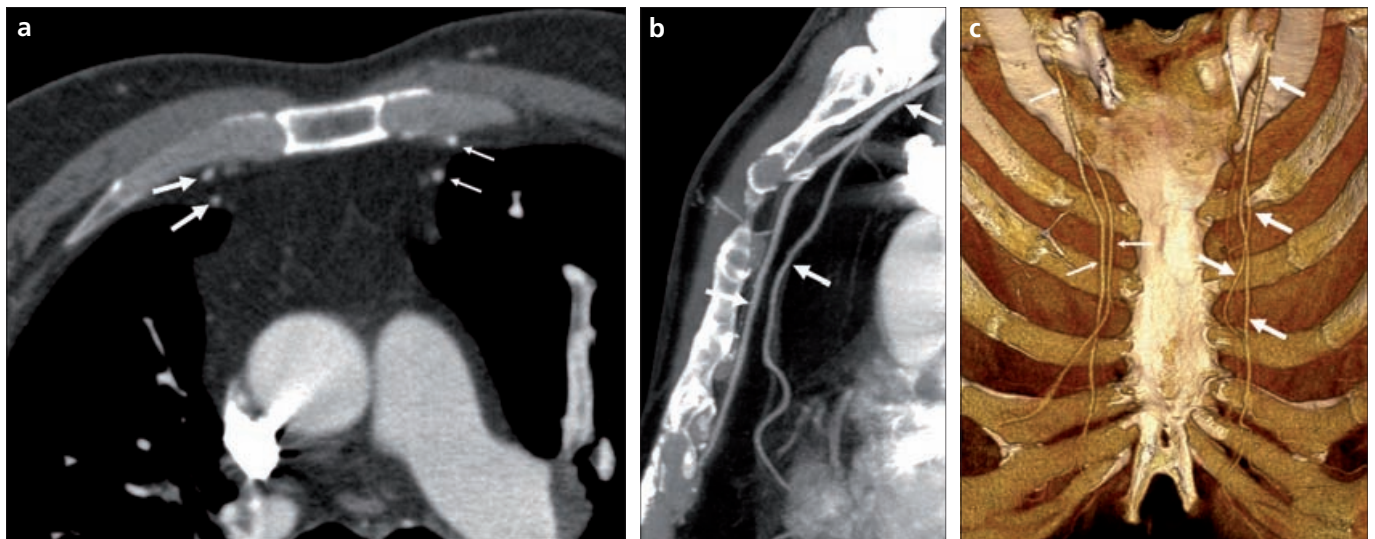
Figure 4. a–c. Axial **(a)**, sagittal MIP **(b)**, and posteroanterior coronal view VR **(c)** CT angiography images show partially duplicated IMAs on both sides in a 62-year-old man. LIMA *(thin arrows)* and RIMA *(thick arrows)* duplicate at the level of the first and second costal cartilage, respectively.
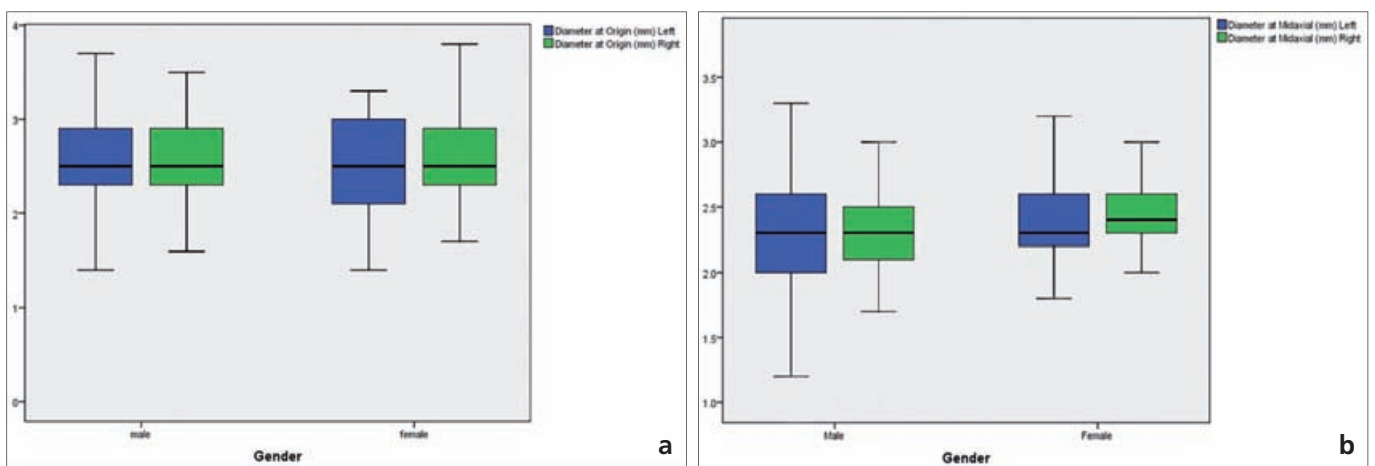
Figure 5. a, b. The relationship between gender and diameter of the LIMA and RIMA at the origin **(a)** and the level of the tracheal bifurcation **(b)** are shown.
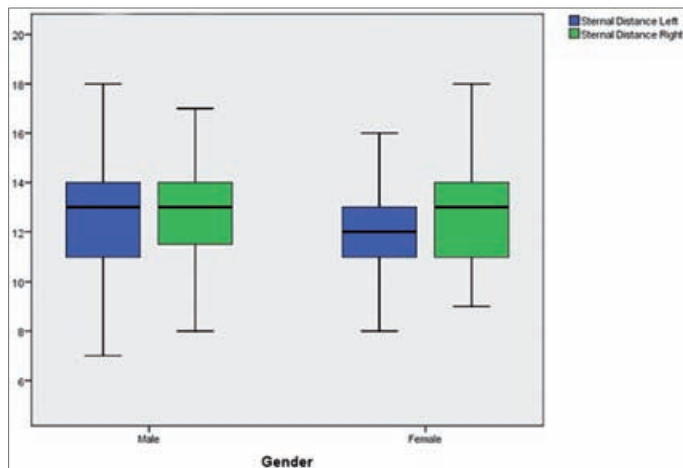
Figure 6. The relationship between gender and the distance to the sternum of the LIMA and RIMA at the level of the tracheal bifurcation is shown.

methods have different advantages and disadvantages. Therefore, different prevalences have been reported for the variation, course, and diameter of both RIMA and LIMA. In anatomic studies, the difficult nature of dissecting the fine caliber vascular structures is a major limitation in detecting the IMA. In angiographic studies, the difficulty of cannulating the fine caliber IMA and the invasiveness of the procedure are major limitations.

Recent developments in the detector technology of MDCT have allowed the depiction of the vascular structures, even the fine caliber ones, with high spatial resolution in a very short time (12–17). Although there is a study investigating the IMA with devices with single detectors (5), these devices have longer acquisition times and higher slice thicknesses than devices with 64 detectors and above. These factors can lead to a reduction of spatial and contrast resolutions of the images and an increase in respiratory and other motion artifacts. MDCT angiography allows the scanning of a large FOV area in a shorter scanning time; 3D analyses with MIP, MPR, and VR techniques; detection of the variations of the IMA; and the measurement of the diameter and distance from the sternum. Despite these important advantages, the X-ray requirement is the most obvious disadvantage of this technique (17).

According to its relationship to the anterior scalene muscle, the subclavian artery is divided into three parts. IMA normally arises from the first part of the subclavian artery. Daseler and Anson (18) found six of the 769

arteries (0.78%), and Vorster et al. (19) found one artery (0.83%) arising from the third part of the subclavian artery. In our study, all of the IMAs arose from the first part of the subclavian artery. The IMA occasionally has a common origin with the other branches of the subclavian artery, such as the thyrocervical trunk, scapular artery, dorsal scapular artery, thyroid artery, or costocervical trunk (6–8). In our study, three (two LIMA and one RIMA) of the 328 arteries (0.91%) had a common origin with the thyrocervical trunk and costocervical trunk. Conversely, the remaining 325 IMAs had an origin separate from the subclavian artery. This finding can be important in cardiovascular bypass surgery. The bypass grafts with LIMA, which have a common origin, must be examined after the surgery. We did not find a variation of the IMA in the literature as seen in our case, shown in Fig. 3. In this patient, two (0.6%) IMAs (one LIMA and one RIMA) in the same patient were partially duplicated at the level of the first and second costal cartilage.

For breast reconstruction with free flaps, the vessels in the axilla are the most common recipient vessels. But after radiotherapy, these vessels tend to be small and vulnerable. In 1980, Harashina et al. (20) reported that the IMA can be used in breast reconstruction with a free groin flap. Hefel et al. (3) reported that with their predictable anatomy and adequate size, the IMA is a suitable artery for free tissue transfer in reconstructive surgery of the thoracic region, especially in breast

reconstruction. In this cadaveric study, they found that the smallest diameter of the artery was 0.99 mm. They also mentioned that the IMA diameter differs significantly in the left and right sides in the female. In our study, with MDCT angiography, we found that the smallest IMA diameter was 1.2 mm. We did not find any differentiation with the right and left sides, or with gender. Furthermore, we did not find a correlation between the diameters of the IMAs and age. This finding is in accordance with Hefel et al. (3) and Dignan et al. (21).

The variations of the origin of the IMA mentioned in the literature (6–8, 18, 19) are located away from the side of surgical approach at the fourth intercostal space and do not interfere with surgery. However, we found two duplicated IMAs (one RIMA and one LIMA) in the same patient at the level of the second rib. This location is very close to the surgical approach, and the surgeon must be aware of the possibility of variations like those in our case.

For the biopsy of pulmonary and mediastinal lesions and the drainage of pleural collections, many interventional physicians recommend the anterior mediastinal approach (22, 23). In this procedure, the inadvertent puncture of the IMA is potentially fatal. Glassberg and Sussman (24) reported two cases of life-threatening hemorrhage due to percutaneous transthoracic interventions in 1990. Oh et al. (4) reported that above the first rib, there is a safe biopsy window on the majority of sides (70.1%). They also mentioned that the vast majority of the IMAs are in contact with the brachiocephalic vein and can be identified from its typical appearance.

Glassberg et al. (5) measured distance to the sternal edge of 100 IMAs on both sides at the level of the aortic arch and main pulmonary artery. They found the mean distance 1.47±0.30 cm on the left and 1.57±0.30 cm on the right side. In their cadaveric study, Hefel et al. (3) found the mean diameter 14.53 mm on the left and 14.97 mm on the right side. In our study, we found the distance between the lateral margin of the sternum and the LIMA or RIMA (at the level of the tracheal bifurcation) ranged from 7 to 18 mm (mean, 12.42 mm; median, 12 mm) and 8 to 21 mm (mean, 13.00 mm; median, 13.01 mm), respectively. For

interventional procedures from the anterior approach, we suggest a diameter greater than 2.2 cm from the lateral margin of the sternum. This value is close to the 2.5 cm that is mentioned by Glassberg et al. (5). In our study, we found that the diameter of the RIMA from the sternal edge was higher than the LIMA ($P < 0.001$), although we believe that this finding is likely to be without major clinical consequences.

Because the artery must be large enough and easily accessible for anastomoses, the IMA diameter is important in breast reconstruction. In our study, we analyzed the CT angiography of the arcus aorta and its branches; thus, we could not demonstrate all side and end branches of the IMA, especially the superior epigastric artery. Henriquez-Pino et al. (25) reported that the pericardiacophrenic artery originated from the IMA in 89% of 100 dissected cadavers.

In conclusion, its important location, adequate size, and predictable anatomy make the IMA a suitable recipient vessel for free tissue transfer, especially in breast reconstruction. Although the LIMA is the artery of choice in coronary artery bypass grafting, we think surgeons must be aware of rarely seen variations. For interventional procedures from the anterior approach, we suggest a distance greater than 2.2 cm from the lateral margin of the sternum to avoid iatrogenic damage of IMAs. For all these considerations, MDCT angiography allows 3D analysis with MIP, MPR, and VR techniques in the demonstration of normal anatomic features. It is also useful for measuring the diameter and distance from the sternum and detecting variations of the IMAs.

Conflict of interest disclosure

The authors declared no conflicts of interest.

References

1. Loop FD, Lytle BW, Cosgrove DM, et al. Influence of the internal-mammary-artery graft on 10-year survival and other cardiac events. N Engl J Med 1986; 314:1–6.
2. Fiore AC, Naunheim KS, Dean P, et al. Results of internal thoracic artery grafting over 15 years: single versus double grafts. Ann Thorac Surg 1990; 49:202–208.
3. Hefel L, Schwabegger A, Ninković M, et al. Internal mammary vessels: anatomical and clinical considerations. Br J Plast Surg 1995; 48:527–532.
4. Oh JK, Han DH, Ko JM. The internal mammary vessels above and below the first rib on multidetector CT: implications for anatomical feasibility of lung biopsy via anterior approach. Diagn Interv Radiol 2011; 17:223–228.
5. Glassberg RM, Sussman SK, Glickstein MF. CT anatomy of the internal mammary vessels: importance in planning percutaneous transthoracic procedures. AJR Am J Roentgenol 1990; 155:397–400.
6. Quain R. The anatomy of the arteries of the human body. London: Taylor and Walton, 1844.
7. Adachi B. Das Arteriensystem der Japaner. Tokyo: Kenkyusha, 1928.
8. Hafferl A. Lehrbuch der topographischen Anatomie. Berlin: Springer, 1969.
9. Ludwig KS. Relation of the superior epigastric artery of the diaphragm and to the transverse muscles of the thorax and abdomen. Acta Anat (Basel) 1955; 25:85–91.
10. Kremer K, Platzer W. Chirurgische Operationslehre. Stuttgart: Thieme Verlag, 1991.
11. Sehovic S, van der Zypen E. The sternocostal triangle and its relationship to the blood vessels of the anterior abdominal wall. Acta Anat (Basel) 1984; 118:231–237.
12. Morita Y, Takase K, Ichikawa H, et al. Bronchial artery anatomy: preoperative 3D simulation with multidetector CT. Radiology 2010; 255:934–943.
13. Hartmann IJ, Remy-Jardin M, Menchini L, Teisseire A, Khalil C, Remy J. Ectopic origin of bronchial arteries: assessment with multidetector helical CT angiography. Eur Radiol 2007; 17:1943–1953.
14. Remy-Jardin M, Bouaziz N, Dumont P, Brillet PY, Bruzzi J, Remy J. Bronchial and nonbronchial systemic arteries at multidetector row CT angiography: comparison with conventional angiography. Radiology 2004; 233:741–749.
15. Yıldız AE, Arıyürek OM, Akpınar E, Peynircioğlu B, Çil BE. Multidetector CT of bronchial and non-bronchial systemic arteries. Diagn Interv Radiol 2011; 17:10–17.
16. Türkvatan A, Biyikoğlu SF, Büyükbayraktar FG, et al. Noninvasive evaluation of coronary artery bypass grafts and native coronary arteries: is 16-slice multidetector CT useful? Diagn Interv Radiol 2009; 15:43–50.
17. Battal B, Akgun V, Karaman B, Bozlar U, Tasar M. Normal anatomical features and variations of bronchial arteries: an analysis with 64-detector-row computed tomography angiography. J Comput Assist Tomogr 2011; 35:253–259.
18. Daseler EH, Anson BJ. Surgical anatomy of the subclavian artery and its branches. Surg Gynecol Obstet 1959; 108:149–174.
19. Vorster W, du Plooy PT, Meiring JH. Abnormal origin of internal thoracic and vertebral arteries. Clin Anat 1998; 11:33–37.
20. Harashina T, Imai T, Nakajima H, Fujino T. Breast reconstruction with microsurgical free composite tissue transplantation. Br J Plast Surg 1980; 33:30–37.
21. Dignan RJ, Yeh T Jr, Dyke CM, Lutz HA 3rd, Wechsler AS. The influence of age and sex on human internal mammary artery size and reactivity. Ann Thorac Surg 1992; 53:792–797.
22. Westcott JL. Percutaneous transthoracic needle biopsy. Radiology 1988; 169:593–601.
23. Merriam MA, Cronan JJ, Dorfman GS, Lambiase RE, Haas RA. Radiographically guided percutaneous catheter drainage of pleural fluid collections. AJR Am J Roentgenol 1988; 151:1113–1116.
24. Glassberg RM, Sussman SK. Life-threatening hemorrhage due to percutaneous transthoracic intervention: importance of the internal mammary artery. AJR Am J Roentgenol 1990; 154:47–49.
25. Henriquez-Pino JA, Gomes WJ, Prates JC, Buffolo E. Surgical anatomy of the internal thoracic artery. Ann Thorac Surg 1997; 64:1041–1045.